Journal of Applied Sciences

ISSN 1812-5654

Journal of Applied Sciences 6 (5): 1074-1081, 2006
ISSN 1812-5654

Transient Analysis of FACTS and Custom Power Devices Using Phasor Dynamics

[1]M.A. Hannan and [2]K.W. Chan
[1]Department of Electrical, Electronic and Systems Engineering, Universiti Kebangsaan Malaysia, Malaysia
[2]Department of Electrical Engineering, The Hong Kong Polytechnic University, Hong Kong SAR, China

Abstract: The objective of the research is to provide the application of Generalized Average models of FACTS device, TCSC and custom power device, DVR for power system transient analysis within dynamic phasor approach. The dynamic phasor models of TCSC and DVR are evaluated through simulation of realistic network model of 3 machines 9 bus WECC system. The continuous-time large signal models of TCSC and DVR under a fault condition captured the phasor dynamics of key wave forms. It is found that the increase transient stability and improve power quality response of dynamic phasor model of TCSC and DVR, respectively are closely hugged with the detail time domain EMTP simulation. Numerical simulation of phasor dynamics with larger size steps through solving differential equation is also faster than that of EMTP. Both EMTP and theoretical framework of dynamic phasor models has been simulated using Simulink/Matlab dynamic system modelling software.

Key words: Dynamic phasor, EMTP, transient stability, TCSC, DVR

INTRODUCTION

The objective of the electric power system is to generate and to distribute power to its consumers in a stable, viable and optimal fashion. Its needs that the system can withstand certain major disturbances of the equipments without severe consequence. This motivates the notion of the transient stability (Perez *et al*., 1994), which is essentially the ability of the system operation to recover its stable operating point without major break ups after a special set of first contingencies. The instability problems is one of the severest fault in power system operation loss of synchronism may cause interruption of power supply in large areas, consequently introduces heavily damage to the distribution network and social life (Shuti *et al*., 1993).

Now days, voltage source power electronic converters are widely used often referred to a flexible AC transmission systems (FACTS) and custom power devices, promise to play an important role in emerging deregulated power system. The FACTS device likewise thyristor controlled series compensation (TCSC) is used in power systems for increasing power transfer capability and enhancement of transient stability or to dampen power oscillations and sub synchronous resonances. Dynamic voltage restorer (DVR) is a custom power device designed specially to improve dynamic response of power quality at distribution or transmission level.

Over the years, for the system equivalent and size of integration steps, the electromagnetic transient program, EMTP concept is universally accepted for simulation of complex power system containing non-linearties, power electronic components and their controllers (Adapa and Reeve, 1988). However, due to the limitation of practical computer storage and computation time, the implementation of a complete representation of a large power system in an electromagnetic transients program is difficult. It has practical restrictions on the extent of ac system that can be incorporated into a detailed simulation including valve by valve switching and discrete control timing (Bui *et al*., 1992).

Periodic steady-state approximations in terms of leading Fourier coefficients is a complex form, called phasor, which is classical technique applications such as power systems, electric machine and switching power electronics. Computationally phasor approximations reduce steady-state analysis to algebraic harmonic balancing equation. Traditional phasor representation is ill equipped to capture non periodic transients, now withstanding quasi steady-state extensions (Gilead, 2001). Moreover, the voltages and currents in the power electronic converters and electric drives are typically periodic, but often non-sinusoidal. This

Corresponding Author: M.A. Hannan, Department of Electrical,
Electronic and Systems Engineering Universiti Kebangsaan Malaysia, Malaysia
Tel: +6-03-89216035 Fax: +6-03-89216146

sinusoidal quasi steady-state approximation is widely used to study electromechanical dynamics and it is almost invariably included in software tools for power systems (Stankovic *et al*., 1999). For faster phenomena, time domain simulations are not only a significant computation burden, but also offer little insight into problem sensitivities to design quantities and no basis for design for protection schemes. This type of fundamental analytical problems is not mitigated by improvements in computational technology (Stankovic *et al*., 2002).

Overcoming the above problems, dynamic phasor has been used successfully to analyze the FACTS equipments-TCSC, UPFC and DVR systems, using its frequency selective approach (Shengli *et al*., 1991). It is well known that the time varying dynamic phasor offers a numbers of advantages over conventional methods. Firstly, it has wider bandwidth in the frequency domain than traditional slow quasi-stationary assumptions. Secondly, dynamic phasor can be used to compute the fast electromagnetic transient with larger step size, so that it makes simulation potentially faster than conventional time domain EMTP like simulation.

For the understanding and control of the interactions among FACTS, custom power device and the utility system, there has been increasing needs for convenient dynamic phasor models that allow fast and accurate transient simulation and improve power quality solutions. However, the model analysis of the FACTS and custom power is challenging because of their hybrid nature, as they incorporate both continuous-time dynamics and discrete events. Therefore, a further demand is imposed on solution algorithms in order to maximize computational speed and numerical efficiency.

In this study, the generalized averaging is applied to obtain the TCSC and DVR phasor dynamics models. The algorithms are applied to the 3 generator 9 bus WECC systems with one TCSC and one DVR installed. The TCSC and DVR models are derived based on the time varying Fourier coefficients that capture the phasor dynamics of the TCSC and DVR. This study indicates that the dynamic phasor model has potential advantages to enhance the power system stability as well as power quality solutions.

PHASOR DYNAMICS IN POWER SYSTEM

The extensive dynamic phasor modeling of large modern power system is to be based on generalized averaging theory, in which a periodic waveform x (•) can be approximated on the line interval (t-T, t) with a Fourier series form (Gilead 2002):

$$x(\tau) = \sum_{k=-\infty}^{\infty} X_k(t)\, e^{jk\omega\tau} \qquad (1)$$

Where, $\omega = 2\pi T$ and $X_k(t)$ is the Fourier coefficient, varies with the time, is called dynamic phasor, which is determined by the following averaging operation,

$$X_k(t) = \frac{1}{T}\int_{t-T}^{t} x(\tau)\, e^{-jk\omega\tau}\, d\tau = \langle x \rangle_k (t) \qquad (2)$$

Where, $\langle x \rangle_k(t)$ is used to denote the averaging operation. A key factor for dynamic phasor development is that the derivative of k-th Fourier coefficient is given by the following expression:

$$\frac{d}{dt}X_k = \left\langle \frac{d}{dt}x \right\rangle_k - jk\omega X_k \qquad (3)$$

This formula can be easily verified using (1) and (2) and integration by parts. Differential equations governing their evolution and derived from the original model and harmonic balancing equations are to be obtained in periodic steady state. Theoretical framework and performance analyzing are to be developed in the form of averaged model involving Fourier coefficients.

The definitions given in (1) and (2) will now be generalized for analysis three phase system. The standard notation, where $a = e^{j(2\pi/3)}$ and $a^2 = \bar{a}$. Then the time domain equation can be written as (Gilead, 2002),

$$\begin{bmatrix} x_a \\ x_b \\ x_c \end{bmatrix}(\tau) = \sum_{t=-\infty}^{\infty} e^{jkw_s\tau} \underbrace{\frac{1}{\sqrt{3}}\begin{bmatrix} 1 & 1 & 1 \\ \bar{a} & a & 1 \\ a & \bar{a} & 1 \end{bmatrix}}_{A} \begin{bmatrix} X_{a,k} \\ X_{b,k} \\ X_{c,k} \end{bmatrix}(t) \qquad (4)$$

where, A is the square transformation matrix. The inverse transform of A can be written as $A^{-1} = A^H$. The coefficients of (4) are as follows:

$$\begin{bmatrix} X_{a,k} \\ X_{b,k} \\ X_{c,k} \end{bmatrix}(t) = A^H \frac{1}{T}\int_{t-T}^{t} e^{-jkw_s\tau} \begin{bmatrix} x_a \\ x_b \\ x_c \end{bmatrix}(\tau)\, d\tau = \begin{bmatrix} \langle x \rangle_{a,k} \\ \langle x \rangle_{b,k} \\ \langle x \rangle_{c,k} \end{bmatrix}(t) \qquad (5)$$

Equation 5 defines 3-phase dynamic phasor at frequency kws. Now the derivatives of k-th Fourier coefficient of Eq. 5 can be written as:

$$\frac{d}{dt}\begin{bmatrix} X_{a,k} \\ X_{b,k} \\ X_{c,k} \end{bmatrix}(t) = A^H \begin{bmatrix} \left\langle \frac{d}{dt}x_a(\tau) \right\rangle k \\ \left\langle \frac{d}{dt}x_b(\tau) \right\rangle k \\ \left\langle \frac{d}{dt}x_c(\tau) \right\rangle k \end{bmatrix}(t) - jkw_s \begin{bmatrix} X_{a,k} \\ X_{b,k} \\ X_{c,k} \end{bmatrix}(t) \qquad (6)$$

It is observed that Eq. 6 is a vector generalization of Eq. 3.

For the validation of the dynamic phasor models of the large modern power system, faster numerical simulation with larger integration steps will first be made through solving differential equation and then compared the dynamic phasor with detailed time domain EMTP simulation as well as standard quasi steady-state transient stability studies using conventional transient stability software.

FACTS AND CUSTOM POWER IN THE SYSTEM

The 3 machines 9 buses WECC system is used to illustrate transient stability and power quality solution using FACTS and custom power device as shown in Fig. 1.

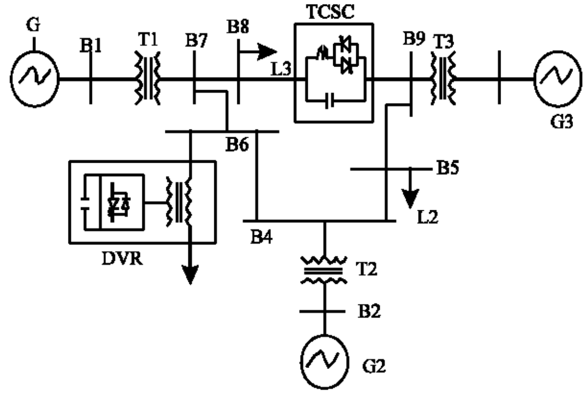

Fig. 1: Basic circuit configuration of 9 bus WECC system including TCSC and DVR

The generalized average models of non-linear loads, transmission lines and 6th order generator model are considered in this system as in (Sanders *et al.*, 1991). In this paper, the dynamic phasor models of FACTS device, TCSC and custom power device, DVR, has been developed. TCSC and DVR are installed in transmission line between bus B8 and B9 and distribution line between bus B6 and load L1, respectively. While TCSC is connected to the system to enhance the transient stability by dampening out power oscillations, DVR is used to improve dynamic response of power quality at transmission or distribution level.

TCSC model dynamics: Dynamic phasor models of TCSC are based on the representation of voltages and currents as time varying Fourier series. Figure 2 shows the circuit diagram of single phase TCSC and its transient waveforms. The system is composed of a fixed capacitor in parallel with a thyristor control reactor. In case of 3-phase TCSC each phase is composed same as single phase TCSC.

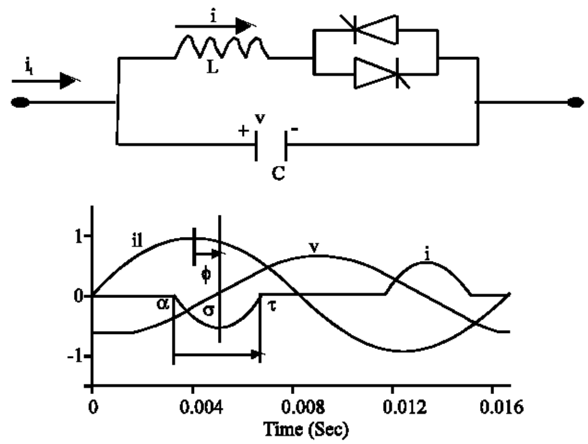

Fig. 2: (a) TCSC circuit diagram (b) Transient waveforms

The capacitor voltage v and reactor current i are natural state variables and the state-space model of TCSC is:

$$C\frac{dv}{dt} = i_l - i$$

$$L\frac{di}{dt} = qv \tag{7}$$

Where, q is a switching function of thyristor that denotes q = 1, when thyristor on and q = 0, when thyristors are off. The dynamics of the phasors V_1 and I_1 are the fundamental Fourier coefficient for v and i

Applying averaging theory of (2) for k = 1, state-space models of (7) become in the form of (3):

$$C\frac{dV_1}{dt} = I_l - I_1 - j\omega_s C V_1$$

$$L\frac{dI_1}{dt} = \langle qv \rangle_1 - j\omega_s L I_1 \tag{8}$$

According the generalized theory (6), Eq. 8 becomes converted into three phase system, as follows:

$$I_{l,abc} = [C_{abc}]\frac{d}{dt}V_{1,abc} - j\omega_s[C_{abc}]V_{1,abc} + I_{1,abc}$$

$$\langle qv_{abc} \rangle_1 = [L_{abc}]\frac{d}{dt}I_{1,abc} + j\omega_s[L_{abc}]I_{1,abc} \tag{9}$$

If $\langle qv \rangle_1$ depended only on the instantaneous values of V_1, I_1, I_l and the control variables, then Eq. 9 would be already state-space form and ready to use and the model

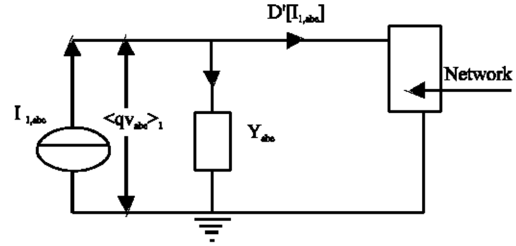

Fig. 3: Dynamic phasor equivalent circuit of TCSC interfacing with network

of the TCSC interfacing with network could be represent as shown in Fig. 3.

However, if Eq. 9 fails to be a state-space model, then switching calculation must be needed for equivalent circuit of TCSC. Therefore, the $\langle qv \rangle_1$ of Eq. 8 can be written as follows (Kundur 1994, Hannan and Chan 2004),

$$\langle qv \rangle_1 = \frac{2}{\pi} \int_{\alpha}^{\tau} v e^{-j\theta} d\theta \tag{10}$$

where, α is a control variable, which depends on the reference conduction angle σ^* and phase angle ξ to the peak line current I_1, by:

$$\alpha = \xi - \frac{\sigma^*}{2}$$

$$\xi = \arg(I_1) \tag{11}$$

where, as τ depends not only phasors and control variables but also the peak value of actual inductor current and phase shift ϕ. Therefore, τ is the function of current phasor I_1,

$$\phi = \arg[-I_1\, I_1]$$

$$\tau = \xi + \frac{\sigma^*}{2} + 2\phi$$

$$\sigma = \sigma^* + 2\phi \tag{12}$$

where σ is the prevailing conduction angle of Thyristor Controlled Reactor (TCR) branch sinusoidal line current. With this assumptions equation (10) can written as:

$$\langle qv \rangle_1 = \frac{1}{\pi} \left[V_1\sigma + V_1 \sin(\sigma) e^{-2j(\xi+\phi)} \right] \tag{13}$$

While the models (8) and (13) are seems to be sufficiently accurate for TCSC operation, it need some refinement for extend its applicable range. The $\langle qv \rangle_1$ in (13) lead the calculation of sinusoidal voltage across the capacitor. This associated sinusoidal steady-state can be determined by setting derivatives to zero in (8) i.e., $dI/dt = 0$, so $I_1 \approx \langle qv \rangle_1 / j\omega_s L_s$. Therefore, a simplified model can be obtained by putting the value of dynamic phasor I_1 into (8),

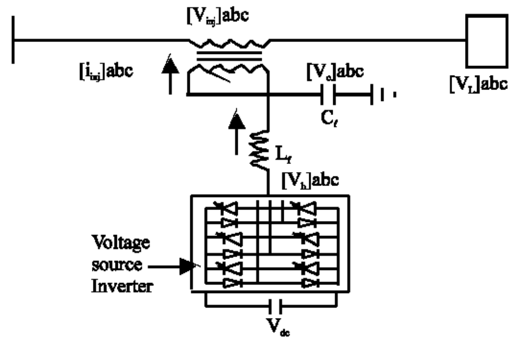

Fig. 4: Basic circuit configuration of DVR

$$C\frac{dV_1}{dt} = I_1 - \frac{\langle qv \rangle_1}{j\omega_s L_s} - j\omega_s C V_1 \tag{14}$$

Now if we consider (14) is an accurate model for TCSC state-space form, because of derivatives of V_1 expressed entirely as the function V_1, I_1 and control variable. Then the phase shift ϕ in (12) can form as:

$$\phi = \arg\left[-I_1\left(\frac{V_1}{j\omega_s L_s}\right)\right] \tag{15}$$

Using (15) when evaluating $\rightarrow \langle qv \rangle_1$ in (14), we obtain an accurate dynamic phasor model of TCSC with V_1 variable. This is a significant simplification.

DVR model dynamics: DVR is a series reactive power compensation device that generates an ac compensating voltage and injects it in series with the supply voltage through an injecting transformer. The main components of a DVR are voltage source inverter, injection transformer, energy storage device and control system. The output of the inverter is connected to an L-C low pass filter, thus to eliminate high frequency harmonics due to switching actions of the inverter. The power circuit configuration of DVR is shown in Fig. 4.

From the circuit configuration, the measured quantity includes $[V_L]_{abc}$, $[V_{inj}]_{abc}$, $[i_b]_{abc}$ and V_{dc}. The DVR required injection voltage obtained by subtracting the measured load voltage $[V_L]_{abc}$, from ideal voltage template. The measured DVR injection voltage $[V_{inj}]_{abc}$, should be transformed to line to phase voltage and resulting voltage is the output L-C filter capacitor voltage $[V_c]_{abc}$. The inverter output current $[i_b]_{abc}$, is measured and the DVR injection current $[i_{inj}]_{abc}$ after the L-C filter is also required to performed the control algorithm. The injection current $[i_{inj}]_{abc}$ is transform from the line to phase current and phase current is name as $[i_c]_{abc}$.

The inverter output voltage $[V_b]_{abc}$ is obtained in terms of inverter modulation index $[m]_{abc}$ and the measured dc-link capacitor voltage as:

$$[V_b]_{abc} = [m]_{abc} V_{dc}/2 \tag{16}$$

By applying the Kirchhoffs current and voltage law, the state-space model of the DVR power system equations are obtained as:

$$C_f \frac{d}{dt}[V_c]_{abc} = [i_b]_{abc} - i_{inj\ abc} \tag{17}$$

$$L_f \frac{d}{dt}[i_b]_{abc} = [V_b]_{abc} - [V_c]_{abc} \tag{18}$$

$$C_{dc} \frac{d}{dt} V_{dc} = i_{dc} - \frac{V_{dc}}{R_{dc}} \tag{19}$$

By applying to the three-phase differential equations, the system average state-space model is derived in the synchronous d-q frame and in components form as:

$$\frac{d}{dt}[V_c]_{dq} = \begin{matrix} 0 & \omega \\ -\omega & 0 \end{matrix} V_{c\ dq} + \frac{1}{C_f}[i_b]_{dq} \frac{1}{C_f}[i_c]_{dq} \tag{20}$$

$$\frac{d}{dt}[i_b]_{dq} = \begin{matrix} 0 & \omega \\ -\omega & 0 \end{matrix} [i_b]_{dq} + \frac{1}{L_f}[V_b]_{dq} \frac{1}{L_f}[V_c]_{dq} \tag{21}$$

Equation 21 can be written by putting the value of $[V_b]_{dq}$ from Eq. 16 as follows:

$$\frac{d}{dt}[i_b]_{dq} = \begin{matrix} 0 & \omega \\ -\omega & 0 \end{matrix} [i_b]_{dq} + \frac{V_{dc}}{2L_f}[m]_{dq} \frac{1}{L_f}[V_c]_{dq} \tag{22}$$

In order to simplify the analysis procedure an assumption has been made that the dc bus parallel resistor is very large, R_{dc} ? infinity i.e. there is no loss at the dc bus. Therefore, average state-space model of dc voltage in the synchronous d-q frame is:

$$\frac{d}{dt} V_{dc} = \frac{3}{2} \frac{1}{C_{dc}} [m]_{dq}^T \ [i_b]_{dq} \tag{23}$$

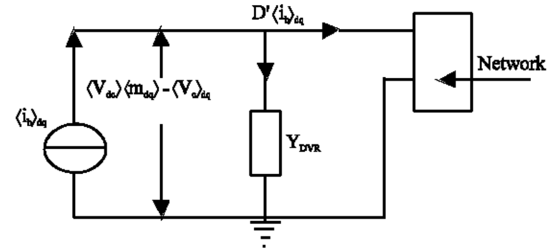

Fig. 5: Dynamic phasor equivalent circuit of DVR interfacing with network

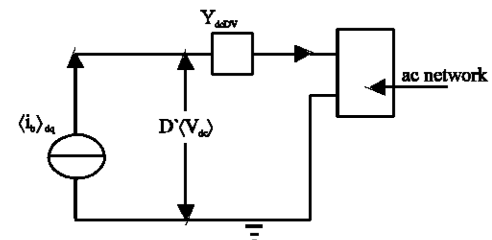

Fig. 6: Dynamic phasor equivalent dc circuit of DVR interfacing with ac network

The input variables are the modulation indices $[m]_{dq}$ and the output variables are the series injection phase voltage $[V_c]_{dq}$. The other state variables are inverter output ac current $[i_b]_{dq}$, dc bus voltage V_{dc} and the series injection current are considered as perturbation.

Dynamic phasor model of Eq. 20, 21 and 23 are derived from time domain model using (3) and (6), in which it will turn out accurate dynamic model of DVR as follows:

$$\frac{d}{dt}\langle V_c\rangle_{dq} = \begin{matrix} 0 & \omega \\ -\omega & 0 \end{matrix} \langle V_c\rangle_{dq} + \frac{1}{C_f}\langle i_b\rangle_{dq} \frac{1}{C_f}\langle i_c\rangle_{dq} \tag{24}$$

$$\frac{d}{dt}\langle i_b\rangle_{dq} = \begin{matrix} 0 & \omega \\ -\omega & 0 \end{matrix} \langle i_b\rangle_{dq} + \frac{1}{2L_f}\langle V_{dc}\rangle \langle m\rangle_{dq} \frac{1}{L_f}\langle V_c\rangle_{dq} \tag{25}$$

$$\frac{d}{dt}\langle V_{dc}\rangle = \frac{3}{2}\frac{1}{C_{dc}} \langle i_b\rangle_{dq} \langle m\rangle_{dq}^T \tag{26}$$

Generalized averaging synchronous reference frame of ac and dc side of DVR model (25) and (26) interfacing can be represent as shown in Fig. 5 and 6. Where Y_{DVR} and Y_{dcDVR} are admittances of model (25) and (26).

Therefore, in a steady state the dynamic phasor model 25) and (26) can be complete equivalent circuit of DVR model. However, it may include PWM control, detail modulation index for a better accuracy, but it will increase more complexity.

RESULTS AND DISCUSSION

This section present the results obtained from dynamic phasor models and EMTP simulation of 3 machine 9 bus system network as shown in Fig. 1, where generator 3 is a slack bus and 3 constant power loads of each 250 MW and 125 MVar were considered. The rating of generator 1, 2 and 3 are 588 MVA, 588 MVA and 5880 MVA, respectively. The field excitation voltage and mechanical power of generators are assumed to be a constant. The injecting transformers of the system with rated 588 MVA and 5880 MVA, 500/13.8 kV and a leakage reactance of 0.01 p.u. were considered. The numerical value of network elements and generator models parameters are used as in (Hannan and Chan 2004).

In TCSC, the switching elements are considered as anti-parallel thyristors. The fixed capacitor and the thyristor controlled reactor of TCSC are assumed to be values of 1.5 μF and 6.8 mH, respectively. The DVR of the system consists of a voltage source inverter, 3 phase transformer rated at 375 MVA, 500/13.8 kV with leakage reactance of 0.1 p.u and a dc capacitance. The optimum size of dc capacitance value is assumed to be 175 μF. A low pass passive filter of reactance and capacitance value as 0.1 p.u and $1.32e^{-3}$ p.u., respectively are considered for

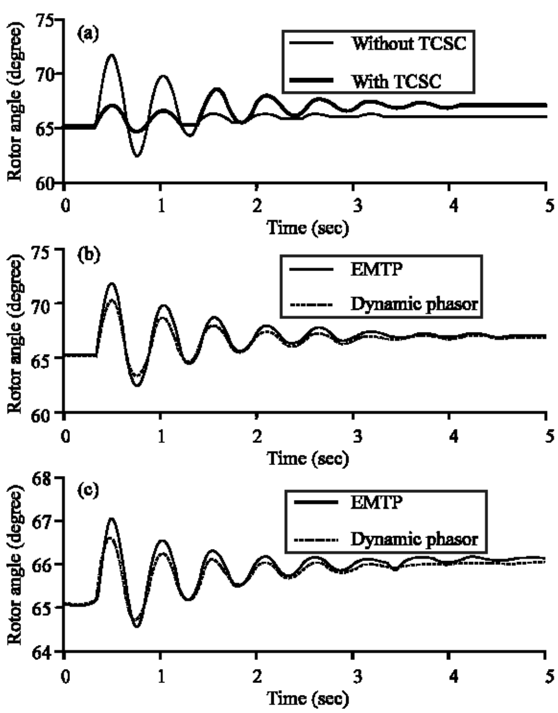

Fig. 7: Generator rotor angle transient a) With and without TCSC b) Without TCSC EMTP and dynamic phasor c) With TCSC EMTP and dynamic phasor

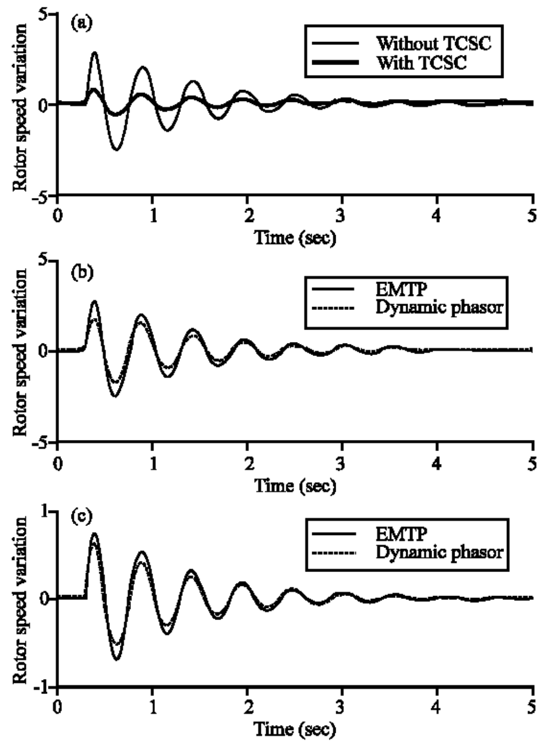

Fig. 8: Generator rotor speed variation a) With and without TCSC b) Without TCSC EMTP and dynamic phasor c) With TCSC EMTP and dynamic phasor

attenuation of high order harmonics generated by voltage source inverter.

For creating transient, a balanced 3-phase to ground fault occurred between DVR and load L1 at 0.3 sec for duration of 100 ms. The EMTP simulation result of subtransient reactance of generator rotor angle without TCSC and with TCSC connected to the system is shown in Fig. 7a. In Fig. 7a, it can be seen that transient stability increased with the aids of TCSC and finally it become almost steady state value at 3 sec. In Fig. 7b and c, the dynamic phasor models behind subtransient reactance of generator rotor angle without and with TCSC connected are closely hug with the EMTP simulation.

Figure 8 shows the generator rotor speed variation of EMTP and dynamic phasor models without and with TCSC connected to the system. The spectrum analysis of this case suggest that TCSC responds well to increase transients stability as well as dynamic phasor models hug the EMTP simulation with quite satisfactory.

In dynamic phasor modeling, the network differential equations are replaced by a set of algebraic equations at a fixed frequency, thus the simulation time reducing dramatically. Figure 9 illustrates the electrical power at generator 1 during transient.

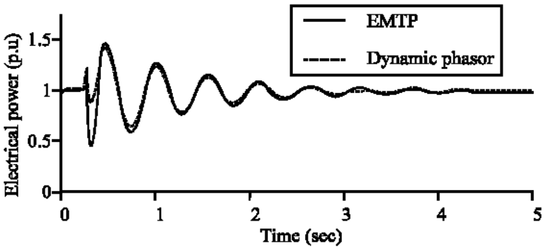

Fig. 9: Electrical power in generator terminal a) Solid line EMTP b) Dotted line dynamic phasor

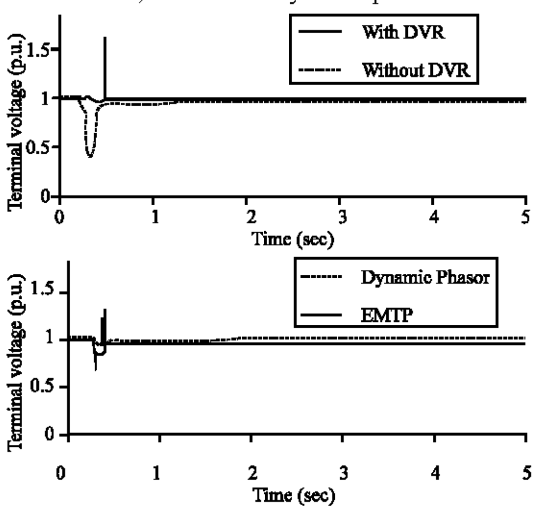

Fig. 10: Generator terminal voltage a) With and without DVR b) With DVR EMTP and dynamic phasor

In particular implementation, it has found that the phasor model is typically 2 or 3 time faster than detail time domain simulation. It can also be seen that with the abrupt transient of EMTP simulation, the phasor models are still able to provide satisfactory agreement of tracking between the waveforms.

Figure 10a illustrates the terminal voltage at bus 1, it is found that without DVR connected, the terminal voltage sag down more than 50% due to 3-phase fault created at 0.3 sec for a duration of 100ms, where fault impedance X/R ratio equal to 1. However, with connected DVR, the sag down voltage is compensated and returns to near its rated voltage. Figure 10b shows the generator terminal voltage of dynamic phasor model and EMTP simulation. We considered here only fundamental components of dynamic phasor model. It can also be seen that there is a spike at the end of the fault in both EMTP and dynamic phasor models. This is due to the switching of voltage source inverter. In this case dynamic phasor model also excellently match with time domain simulation.

In order to simulate generator swing dynamics, Fig. 11a shows that the phase A voltage at load 3 is modulated at 10° phase shift during 0.2 s to 0.24 s

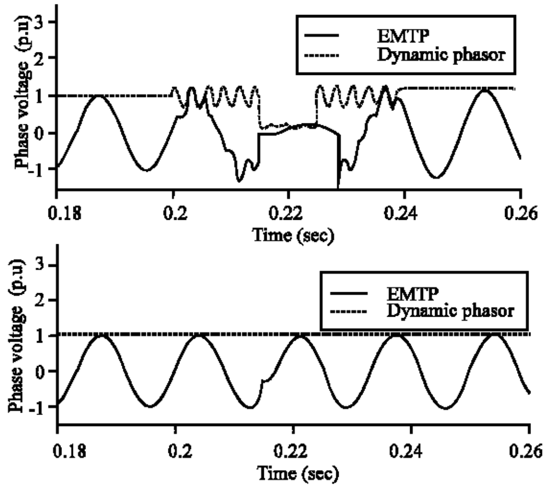

Fig. 11: Voltage at load 3 EMTP and dynamic phasor simulation a) Without DVR b) With DVR

between DVR output voltage, $[V_b]_{abc}$ and network voltage, where firing angle is 60°. The 3-phase to ground fault occurred at 0.215 s for a duration of 10 ms. It can be seen from Fig. 11a that due to modulation there are some harmonics in both the EMTP and dynamic phasor simulation. It can also be seen that the rms value of dynamic phasor models recover at the end of fault period, where as in case of EMTP, fault recovering process has to wait until zero crossing of the phase voltage occurs. In Fig. 11b, the sag down voltage is compensated by DVR and with the aid of low pass LC filter of DVR, voltage harmonics are also eliminated. However, in both cases, without and with DVR, the rms values of dynamic phasor model are still able to provide satisfactory agreement of tracking between the waveforms of the time domain and dynamic phasor models.

CONCLUSIONS

Dynamic phasor models capture transients in fundamental harmonic coefficients of the system network. In this paper, the dynamic phasor models of FACTS device, TCSC and custom power device, DVR, were developed using the methodology of average generalized technique. Their performance has been fully evaluated using a modified 3 machines 9 bus WECC system. Test results obtained from the dynamic phasor simulation and detail time domain simulation illustrated that dynamic phasor models can faithfully represent the transient behaviors of the switching devices and can be used to analyze the transient operations of model power systems with embedded FACTS and custom power device. While the accuracy of dynamic phasor simulation is close to the detail time domain simulation, it has a faster simulation speed due to the use of larger integration steps.

ACKNOWLEDGMENTS

The authors gratefully acknowledge the support of the Hong Kong Polytechnic University under Project G-T732 and A-PA2L.

REFERENCES

Adapa, R. and J. Reeve, 1988. A new approach to dynamic analysis of ac networks incorporating detailed modeling of DC systems. Part II: Application to Interaction of DC and Weak AC Systems. IEEE Transactions on Power Delivery, 3: 2012-2019.

Bui, L.X., G. Mortin and J. Reeve, 1992. EMTP TACS-FORTAN interface development for digital controls modeling. IEEE Transactions on Power Systems, 7: 314-319.

Gilead, T., 2002. On approximate phasor models in dissipative bilinear systems. IEEE Transactions on Circuits and Systems-1: Fundamental Theory and Applications, 49: 1167-1179.

Gilead, T., 2001. Phasor models in bilinear dissipative systems. The Proceedings of the 40th IEEE Conference on Dicision and Control, Oriando, USA, pp: 459-460.

Hannan, M.A. and K.W. Chan, 2004. Modern power systems transients studies using dynamic phasor models. The Proceeding of IEEE International Conference on Power System Technology-POWERCON, Singapore, 2: 1469-1473.

Kundur, P., 1994. Power system stability and control. New York: McGraw Hill.

Perez, L.G., A.J. Flechsig and V. Venkatasubramanian, 1994. Modelling the protective system for power system dynamic analysis. IEEE Transactions on Power Systems, 9: 1963-1973.

Stankovic, A.M., S.R. Sanders and T. Aydin, 2002. Dynamic phasor in modeling and analysis of unbalanced polyphase AC machines. IEEE Transactions on Energy Conversion, 17: 107-113.

Stankovic, A.M., B.C. Lesieutre and T. Aydin, 1999. Modeling and analysis of single phase induction machines with dynamic phasors. IEEE Transactions on Power Systems, 14: 9-14.

Shuti, F., H. Jiaxiao, N. Yixin, C. Jianlin, X. Youfang and Z. Zunlin, 1993. A practicle on-line transient stabil;ity program. IEEE International Conference on Advances in Power System Control, Operation and Management, Hong Kong, pp: 884-886.

Shengli, H., S. Ruihua and X. Zhou, 1991. Anlaysis of balanced and unbalanced faults in power systems using dynamic phasors. IEEE Transactions on Power Electronics, 6: 1550-1556.

Sanders, S.R., J. Noworolski, M. Xiaojun, Z. Liu and G. C. Verghese, 1991. Generalized averaging method for power conversion circuits. IEEE Transactions on Power Electronics, 6: 251-259.